COMPARATIVE STUDY ON SINGLE- AND DOUBLE-PASS CONFIGURATIONS FOR SERIAL DUAL-STAGE HIGH CONCENTRATION EDFA

A.A. Latiff[1], Z. Zakaria[2], A. Jaafar[3], Hazli Rafis[4], V.R. Gannapathy[5]

[1,2,3,4,5] Centre for Telecommunication Research and Innovation (CeTRi),
Faculty of Electronics and Computer Engineering,
Universiti Teknikal Malaysia Melaka (UTeM),
Hang Tuah Jaya, 76100 Durian Tunggal, Melaka, Malaysia.
anasabdullatiff@utem.edu.my

Abstract

A comparative study on a single- and double-pass configurations for Erbium-doped fiber amplifier (EDFA) are demonstrated using a gain media of high concentration Silica-based erbium doped fiber (EDF). The amplifier has two stages comprising a 1.5 m and 9 m long EDF optimized for C-band and L-band operations respectively, in a single-pass and double-pass configurations. The CFBG is used at the end of EDF stage to allow a double propagation of signal and thus increases the attainable gain in both C- and L-band spectra. At an input signal power of -30 dBm, a flat gain of 22 dB is achieved with a gain variation of ±3 dB within a wide wavelength range from 1530 to 1600nm (C- and L-band) in double-pass configurations. The corresponding noise figure varies from 4 to 8 dB within this wavelength region. The flat gains for single-pass configuration only amplify within 1555 nm to 1600 nm (L-band).

Index Terms: *double-pass amplifier, single-pass amplifier, serial dual-stage amplifier, silica based Erbium.*

----------***----------

1. INTRODUCTION

Dual-stage erbium-doped fiber amplifier (EDFA) have been attracted a lot of researches and scientists around the world due to their advantages having a wideband amplifications within 1530 nm to 1600 nm. These significant advantages lead to enormous bandwidth and consistency in connectivity, thus make an optical fiber communication system to be used widely as a backbone in world telecommunication system. In improving the performance of light amplification, various gain medium materials such as such as Tellurite[1, 2] multi-component Silicate[3, 4], and Bismuth Oxide based glass[5] have been proposed. However, the gain spectrum of these amplifiers still remains non-uniform with the variation of wavelength. On other hand, researchers also proposed various configurations amplifier[6, 7] which include serial and parallel dual-stage EDFAs. The serial dual-stage EDFA have better gain flatness compare to parallel dual-stage EDFA[8].

In this paper, we compare the amplifiers performance obtained in single-pass and double-configurations for serial dual-stage EDFA. A silica-based EDFA is demonstrated to operate in C- and L-band regions. The serial dual-stage amplifier employs two pieces of gain medium in single-pass and double-pass configurations. A chirp fiber Bragg grating (CFBG) is incorporated in each stage to allow the double-pass operation. In the design of EDFAs, it is necessary to determine optimization of amplifier parameters such as the optimal fiber length, pumping wavelength, and pumping power, accordingly to obtain a maximum gain or bandwidth of the EDFA. The experimental results are also compared to the simulation results[9], which are obtained using GainMaster™ software. Insertion losses have been incorporated in the simulation.

2. EXPERIMENTAL SETUP

The serial dual-stage amplifier in single-pass and double-pass configurations are shown in Figure 1 (a) and (b), which utilizes a Silica-based EDF as a gain medium and CFBG as a reflector. The gain medium is a highly doped fiber with Erbium ion concentration of 2200 ppm, where the length is fixed at 1.5 m and 9 m for C-band and L-band operation, respectively. Two forward pump laser at 1480 nm with optimum output power of 150 mW and 60 mW are deployed in C-band and L-band stages respectively. A wavelength division multiplexed (WDM) coupler is used to combine the pump light with the signal at each stage. Figure 1(a) shows the EDFA employing serial dual-stage EDFs in single-pass configuration. The single-pass amplifier performance was obtained by measuring the amplified signal at the output end of second-stage EDF. The single-pass amplifier performance is then compared to the double-pass amplifier. The double-pass amplifier was obtained by placing the C-band and L-band CFBGs at the each output end of EDF stage as shown in Figure 1(b). The C-band CFBG is placed midway the two stages to act as a reflector for the C-band EDFA. It reflects C-band signal for double-pass operation and pass-through the L-band signal to be transmitted so that it can be

amplified by the second stage of the amplifier. The insertion loss of the WDM couplers is assumed to be 0.9 and 1.8 dB in the C- and L-band spectra, respectively. In this experiment, the gain and noise figure of both EDFAs were characterized from 1520 nm to 1620 nm at 5 nm step size using a tunable laser source (TLS) used in conjunction with an optical spectrum analyzer (OSA). The performances of the EDFAs are investigated for two input signal powers: -30dBm and 0dBm.

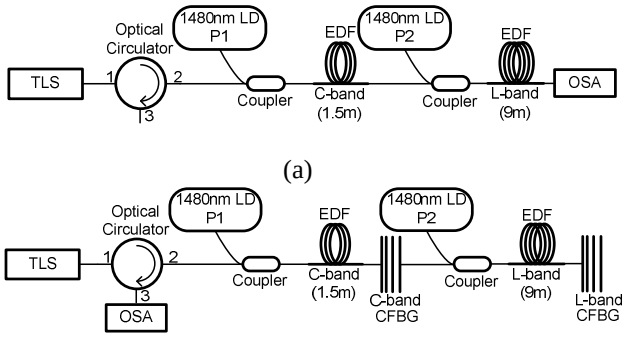

Fig -1: Configuration of serial dual-stage EDFA in (a) single-pass and (b) double-pass.

Figure 2 shows the transmission spectra of both CFBGs used in double-pass configuration. As shown in the figure, the C-band CFBG has a reflectivity of more than 90% centered at the wavelength of 1545 nm with a bandwidth of about 40 nm while the L-band CFBG has a reflectivity of more than 98% centered at 1592 nm with a bandwidth of about 50 nm.

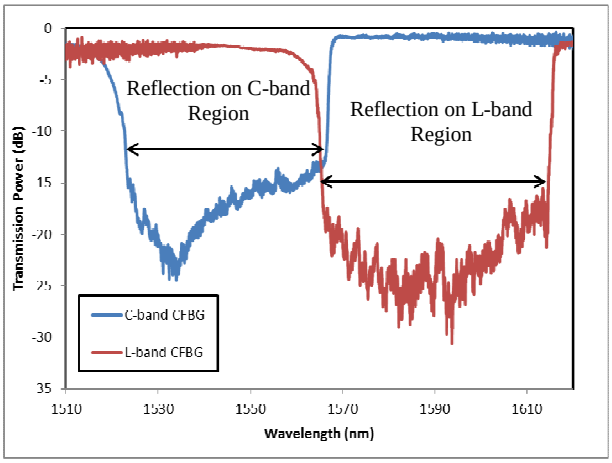

Fig -2: Transmission spectra of the CFBGs for C- and L-band for double-pass configuration.

3. PUMP POWER AND OPTIMIZATION

First, the optimum pump power is investigated for both C-band and L-band EDFAs. Figures 3 (a) and (b) show the gain and noise figure characteristics of the single-pass and double-pass amplifiers against pump power for the C-band and L-band operations, respectively at both input signal powers of -30 dBm and 0 dBm. In the experiment, the TLS is fixed at 1550 nm (C-band) and 1590 nm (L-band) and the 1480 nm pump power is varied from 20 to 185 mW for both single-pass and double-pass amplifiers. As shown in Figure 3 (a), the small input signal power (-30 dBm) of double-pass amplifier shows the saturated gain occurs when the pump power is increased from 120 mW to 170 mW. For the single-pass amplifier, their small signal gain is saturated as the pump power increase from 80 mW to 170 mW. Both single-pass and double-pass amplifiers share the same behavior where the gain start drop when the pump power increase from 170 mW onwards. At high input signal power (0 dBm), the single-pass and double-pass amplifier gains are increased proportionally to pump power level from 20 mW and saturated at 150 mW. From the observation, the high input signal power requires more pump power level as compared to small signal power in achieving saturation effect and thus an optimum gain performance. As shown in the Figure 3 (b), the small input power shows the saturated gain occurs when the pump power is increased from 80 mW for single-pass and double-pass amplifiers. At high input signal power, the gain for single-pass and double-pass amplifiers are increased proportionally to pump power level from 20 mW to the maximum limit of 185 mW. It is shown that the threshold pump power is higher in the L-band compared to that of C-band EDFA. This is attributed to the L-band EDFA, which uses a longer length of EDF (9m) and thus a higher power of pump is required to achieve a population inversion in L-band region. As a result, the pump power of 150 mW obtains the most flat gain for C-band and L-band regions.

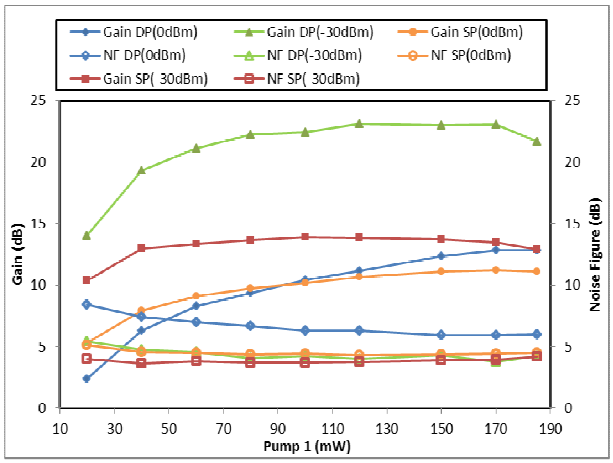

Fig -3: Characterization of pump power for single-pass and double-pass configurations at (a) C-band (1550 nm) and (b) L-band (1590 nm) regions.

After optimizing the pump power , the combination of pump powers in serial dual-stage is investigated. Figure 4 shows the ASE spectra of serial dual-stage EDFA in single-pass and double-pass configurations at 1480 nm pump power combinations. As shown in this figure, the optimum ASE spectrum is obtained at pump power combination of 150 mW and 60 mW for C-band and L-band pump power respectively, which can translate to flat gain and low noise figure operations for the amplifier. At these optimum pump powers, the lasing action at wavelength within 1560 nm to 1570 nm region is minimum and thus more energy can be converted to gain.

At pump power of 150 mW for both C-band and L-band stages, the EDFA shows the gain suppression at C-band region. By reducing the second-stage pump power up to 60 mW, the gain at C-band region improves and lasing action minimizes. Thus, pump power of 60 mW is appropriate for single-pass and double-pass amplifiers in achieving high ASE with minimum lasing action. On the other hand, the single-pass amplifier can practically be operated within 1555 to 1600 nm due to the higher ASE power. The double-pass EDFA configuration in this experiment is equivalent to the close-loop laser configuration. In addition, the intersection of CFBG transmission power expresses atoms at higher population inversion. Therefore, lasing action is approximately stimulated at 1566 nm especially for dual-stage amplifier as shown in Figure 4. In addition, lasing action also induces from the reflections of fiber splices, or from liner or nonlinear scattering in the optical fiber. This lasing action can be controlled by optimizing the pump power, where the lasing action can be minimized in the dual-stage amplifier. However, lower pump power can reduce the gain amplification.

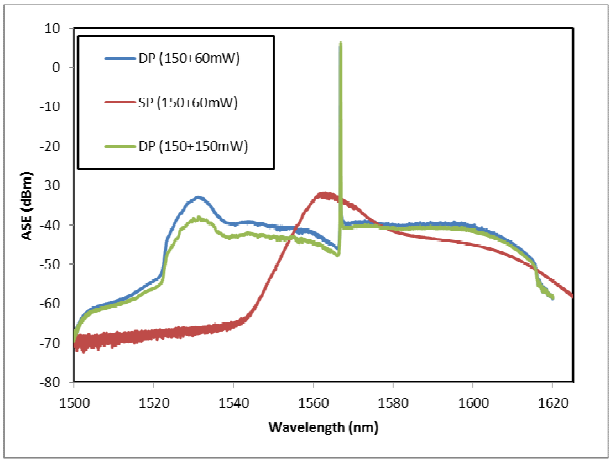

Fig -4: ASE spectra of the EDFA in single-pass and double-pass configurations for C-band and L-band operations.

4. RESULTS AND DISCUSSION

Figures 5 (a) and (b) compare the measured gain and noise figure characteristics between the single-pass (SP) and double-pass (DP) amplifiers. The ASE of single-pass amplifier is also compared with that of the double-pass amplifier. In the experiment, the 1480 nm pump powers are fixed to 150 mW and 60 mW for C-band and L-band stages respectively, while input signal powers are fixed at -30 dBm and 0 dBm. As shown in the figure, wideband operation is achieved in serial double-pass amplifier which operates in wavelength region from 1530 nm to 1600 nm (C- and L-band). However, the single-pass amplifier is successfully operated within 1550 to 1600 nm.

Figure 5 (a) shows the gain at 1565 nm for single-pass amplifier is higher compared to the double-pass amplifiers. The input signal power of -30 dBm within the C-band region shows the average gain of the double-pass amplifier is maintained at 22 dB with a gain variation of ±3 dB, while within the L-band region a lowest gain is maintained at 19 dB with a gain variation of ±0.5 dB. As shown in the figure, the corresponding noise figure is varied within 4 to 8 dB. The average gain of the single-pass amplifier is approximately 18 dB with a gain variation of ±3 dB within 1555 to 1600 nm (L-band). The gain is lower in single-pass amplifier compared to the double-pass amplifier due to the decrease in effective length of gain medium. The spectral bandwidth of single-pass amplifier is approximately 45 nm with the noise figure varying from 4 to 9 dB.

Figure 5 (b) shows the gain in L-band is slightly higher in double-pass amplifier compared to the single-pass amplifier. The average gain of the double-pass amplifier with input signal power of 0 dBm is maintained at 11 dB within the C-band region with a gain variation of ±0.7 dB. Besides that, within the L-band region the double-pass amplifier shows a slightly higher gain at 12 dB with a gain variation of ±0.9 dB compared to single-pass amplifier. The effect of transition within C-band and L-band regions are caused by different level in gain. The corresponding noise figure is varied within 8 dB to 12 dB. While, the average gain of the single-pass amplifier is approximately 10.5 dB with a gain variation of ±0.6 dB within 1555 to 1600 nm. The single-pass amplifier gain is more flatness compared to double-pass amplifiers with the noise figure varies from 4 to 9 dB.
The double-pass amplifier with the input signal power of -30 dBm shows the average optimum flat gain at 22 dB with a gain variation of ±3 dB and the noise figure is varied within 4 to 8 dB. The consequences of progressive absorption in I-25 EDF, the progressive emission of single-pass and double-pass amplifiers have been affected. Therefore, the higher peak gain is induced at 1530 nm.

The EDFA gain spectrum as shown in Figure 5 is produced by two-level system of amplification. Thus, the conventional wavelength spectrum approximately at 1565 nm and long wavelength spectrum from 1610 nm onwards have small ground level absorption corresponding to this laser system. Indeed, as population inversion is decreased, the two-level

system becomes progressively transparent at those wavelengths.

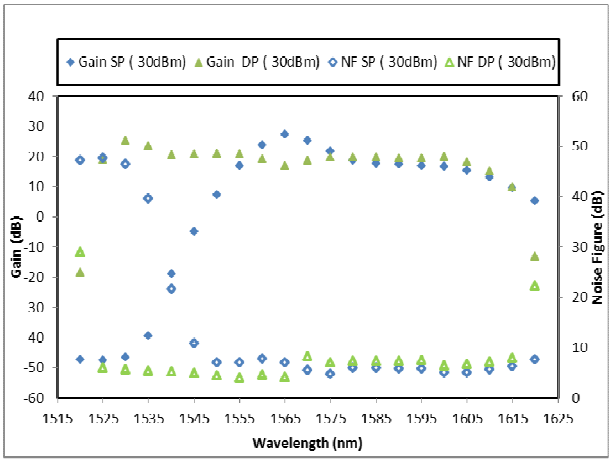

(a)

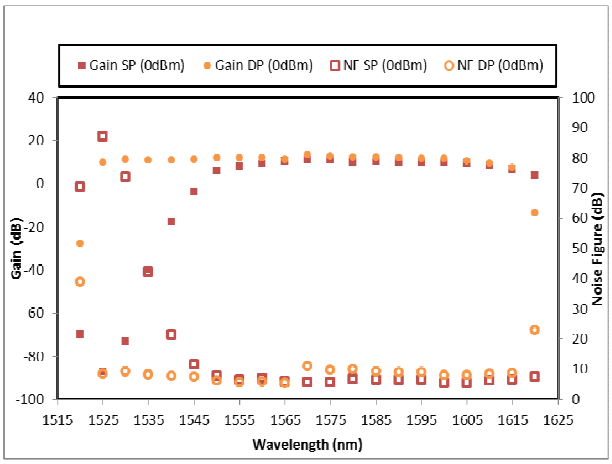

(b)

Fig -5: Comparison of measured gain (solid symbol) and noise figure (hollow symbol) performances between the single-pass and double-pass configurations for EDFA at input signal power of (a) -30 dBm and (b) 0 dBm.

Preliminary design and analysis are done by using commercially available GainMaster Version 1.1. Figures 6 (a) and (b) compare the gain and noise figure characteristics of single-pass amplifier between the experiment and simulation. All required components are dragged and dropped on the blank worksheet interface. Those component parameters are accordingly set as the experimental EDFA single-pass configuration. However, this simulation tool is not compatible to the double-pass configuration.

Figure 4.5 (a) shows that the gain is lower in the experimental amplifier compared to the simulated amplifier with similar plotting pattern. As shown in the figure, the input signal power of -30 dBm demonstrates the experimental average gain decreases as 8 dB in single-pass amplifier due to the losses in the experimental setup. The noise figure is slightly higher in the experimental amplifier compared to the simulated amplifier with similar plotting pattern. The experimental noise figure increase as 1 dB in single-pass amplifier.

Figure 4.5 (b) shows the gain is slightly higher and more flatness in the experimental amplifier compared to the simulated amplifier. As shown in the figure, the input signal power of 0 dBm demonstrates the experimental average gain enhances as 3 dB in serial single-pass amplifier. The simulated amplifier also shows the simulated gain is starting to flat at 1575 nm in single-pass amplifier. The noise figure is slightly lower in the experimental amplifier compared to the simulated amplifier. The experimental noise figure enhances as 1 dB in single-pass amplifier within the wavelength region of flat gain.

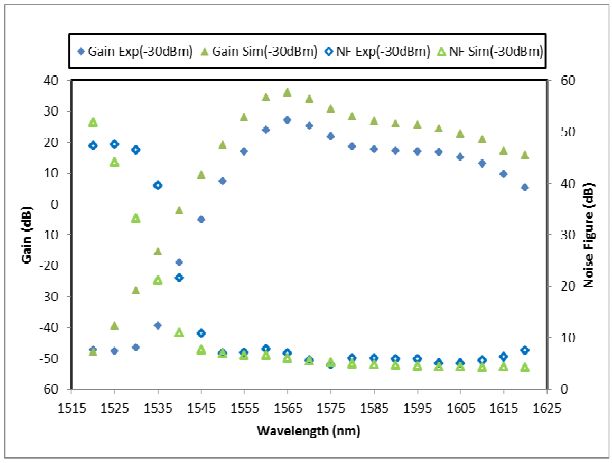

(a)

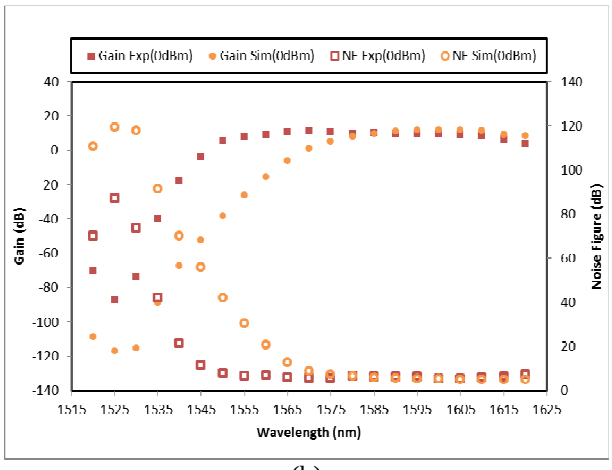

(b)

Fig -6: Comparison of simulated gain (solid symbol) and noise figure (hollow symbol) performances in single-pass configuration for EDFA at input signal power of (a) -30 dBm and (b) 0 dBm.

CONCLUSION

The performances of the serial dual stage EDFA in single-pass and double-pass configurations are demonstrated with EDF length of 1.5 m and 9 m for C-band and L-band operation, respectively. A CFBG is used in both C-band and L-band stages to allow a double pass operation and increase the attainable gain. At input signal power of -30 dBm, the average flat-gain of 22 dB with variation of ±3 dB is achieved within wavelength region from 1530 nm to 1600 nm (C- and L-band). The corresponding noise figure varies

from 4 to 8 dB over this wavelength region. The obtained results for single-pass configuration reveal that experimental and simulated results are in close agreement. Compared to a single-pass amplifier, the flat gain and bandwidth as well as noise figure of the double-pass amplifier are better. However, the optimum flat gain of 0 dBm signal input power requires a higher pump powers which is not available in our laboratory during the experiment.

ACKNOWLEDGEMENT

The authors would like to take this opportunity to thanks those who are contributes directly or indirectly in completion of this article especially Professor Sulaiman Wadi Harun. In addition, the authors also would like to express our gratitude to Universiti Teknikal Malaysia Melaka (UTeM) for the support and encouragement.

REFERENCES

[1] Y. Ohishi, A. Mori, M. Yamada, H. Ono, Y. Nishida, and K. Oikawa, "Gain characteristics of tellurite-based erbium-doped fiber amplifiers for 1.5-µm broadband amplification," *Optics letters*, vol. 23, pp. 274-276, 1998.

[2] S. Shen, M. Naftaly, and A. Jha, "Tungsten–tellurite—a host glass for broadband EDFA," *Optics communications*, vol. 205, pp. 101-105, 2002.

[3] S. Harun, M. C. Paul, N. Huri, A. Hamzah, S. Das, M. Pal, *et al.*, "Double-pass erbium-doped zirconia fiber amplifier for wide-band and flat-gain operations," *Optics & Laser Technology*, vol. 43, pp. 1279-1281, 2011.

[4] A. Ellison, J. Dickinson, D. Goforth, D. Harris, J. Kohli, J. Minelly, *et al.*, "Hybrid erbium silicate conventional-band fiber amplifier with ultra-low gain ripple," in *Optical Amplifiers and Their Applications*, 1999.

[5] X. Cheng, B. Hamida, A. Naji, H. Arof, H. Ahmad, and S. Harun, "Compact and wide-band bismuth-based erbium-doped fibre amplifier based on two-stage and double-pass approaches," *IET optoelectronics*, vol. 6, pp. 127-130, 2012.

[6] S. W. Harun, N. K. Saat, and H. Ahmad, "An efficient S-band erbium-doped fiber amplifier using double-pass configuration," *IEICE Electronics Express*, vol. 2, pp. 182-185, 2005.

[7] B. Hamida, A. Latiff, X. Cheng, M. Ismail, W. Naji, S. Khan, *et al.*, "Flat-Gain Single-Stage Amplifier Using High Concentration Erbium Doped Fibers in Single-Pass and Double-Pass Configurations," in *Photonics and Optoelectronics (SOPO), 2012 Symposium on*, 2012, pp. 1-5.

[8] B. Hamida, A. Latiff, X. Cheng, M. Ismail, W. Naji, S. Khan, *et al.*, "Wideband and flat-gain amplifier using high concentration Erbium doped fibers in series double-pass configuration," in *Computer and Communication Engineering (ICCCE), 2012 International Conference on*, 2012, pp. 109-112.

[9] M. N. S. Zainudin and M. M. Ismail, "Numerical Method Approaches in Optical Waveguide Modeling," *Applied Mechanics and Materials*, vol. 52, pp. 2133-2137, 2011.

BIOGRAPHIES

Anas Abdul Latiff received the B.Eng in electrical from Universiti Tun Hussein Onn Malaysia, and the M.Eng degree in telecommunication from University of Malaya, Kuala Lumpur, Malaysia. He is currently a Lecturer with the Department of Telecommunication Engineering, Universiti Teknikal Malaysia Melaka. His current research interests include electronics, photonics and fiber optic devices.

Dr. Zahriladha Zakaria, PhD, MIEEE, BEM, Grad IEM is currently working as a lecturer at the Faculty of Electronic and Computer Engineering, Universiti Teknikal Malaysia Melaka. (UTeM). His research interests include a variety of microwave device development such as planar and non-planar microwave filters, amplifiers and antennas.

Anuar Jaafar received the B.Eng in electronics from Universiti Teknikal, Malaysia Melaka, and the M.Sc degree in electronic system design engineering from Universiti Sains Malaysia, Penang, Malaysia. He is currently a Lecturer with the Department of Computer Engineering, Universiti Teknikal Malaysia Melaka. His current research interests include electronics, embedded system, and digital systems.

Hazli Rafis Abdul Rahim received the B.Eng in industrial electronic from Kolej Universiti Teknikal Malaysia Melaka, and the M.Eng degree in biomedical from University of Malaya, Kuala Lumpur, Malaysia. He is currently a Lecturer with the Department of Industrial Electronics, Universiti Teknikal Malaysia Melaka. His current research interests include electronic system and biophotonics.

Vigneswara Rao Gannapathy currently serving as a lecturer in Universiti Teknikal Malaysia Melaka (UTeM) and he actively involves in research activities which is related to electronics and wireless networking. His research direction has focused on Wireless Mesh Networks which emerged as a key technology for next-generation wireless networking.